

## Covalent Conjugation of Multi-walled Carbon Nanotubes with Proteins

Changqing Yi, Suijian Qi, Dawei Zhang, and Mengsu Yang

**Abstract** Linkage of proteins to carbon nanotubes (CNTs) is fundamentally important for applications of CNTs in medicinal and biological fields, as well as in biosensor or chemically modulated nanoelectronic devices. In this contribution, we provide a detailed protocol for the synthesis and characterization of covalent CNT-protein adducts. Functionalization of multiwalled carbon nanotubes (MWCNTs) with proteins has been achieved by the initial carboxylation of MWCNTs followed by amidation with the desired proteins. Attenuated total reflection Fourier transform infrared (ATR-FTIR) and X-ray photoelectron spectroscopy (XPS) measurements validated the presence of a covalent linkage between MWCNTs and proteins. The visualization of proteins on the surface of MWCNTs was furthermore achieved using atomic force microscopy (AFM). The protein-conjugated nanocomposites can also be assembled into multidimensional addressable heterostructures through highly specific biomolecular recognition system (e.g., antibody–antigen).

**Keywords:** Carbon nanotubes, Covalent conjugation, Protein, Antibody, ATR-FTIR, XPS, AFM

---

### 1. Introduction

The unique properties of nanomaterials (NMs) in combination with the biorecognition abilities of proteins offer particularly exciting opportunities in molecular imaging (1–3), therapy (4, 5), biomolecule delivery (6, 7), and design of functional nanodevices (8–12). The loss or retention of the native structure of proteins upon their conjugation onto NMs provides an additional variable for controlling NM assembly – intercomponent spacing (13). Though biomolecules, such as DNA and proteins, can be linked to nanotubes *via* noncovalent interactions (14, 15), the use of covalent chemistry is expected to provide better stability, accessibility, and selectivity (16, 17).

Herein, we report a protocol for covalent conjugation of proteins to carbon nanotube (CNT) surface, which has been achieved by the initial carboxylation of CNTs followed by amidation with the desired proteins. This two-step chemical method employs mild conditions and results in tethering of the organic functionality through a covalent bond. This protocol can also be employed to functionalize CNTs with various proteins and amines, including primary amines and secondary amines. The protein-conjugated nanocomposites can be further assembled into multidimensional addressable heterostructures through highly specific biomolecular recognition system, such as antibody-antigen interaction.

---

## 2. Materials

### 2.1. Carboxylation of MWCNTs

1. Pristine MWCNTs, prepared by the chemical vaporization deposition (CVD) method (Nanotech Port, China).
2. 10- $\mu$ m pore size PTFE filter paper (Advantec MFS, Inc.).
3. Ultrasonic cleaning bath (Electron Microscopy Sciences).

### 2.2. Amidation

1. Mouse monoclonal IgG (Santa Cruz Biotechnology).
2. 1-ethyl-3-(3-dimethyl-aminopropyl) carbodiimide (EDC) (Sigma-Aldrich).
3. *N*-hydroxysuccinimide (NHS) (Sigma-Aldrich).
4. Phosphate buffer solution (PBS): 0.1 mol/L, pH 7.4.

### 2.3. Equipment

1. Transmission electron microscope (TEM), Tecnai 12 (Philips).
2. Copper grids with formvar film (Electron Microscopy Sciences).
3. ULVAC-PHI 5802 XPS system (Kanagawa, Japan).
4. FTIR spectrometer Spectrum One (Perkin Elmer).
5. FTIR microscope equipped with a HgCdTe detector cooled with liquid nitrogen (i-Series).
6. Multimode atomic force microscope (Veeco Instruments).

---

## 3. Methods (See Notes 1 and 2)

### 3.1. Carboxylation

1. Pristine MWCNT powder was oxidized in a 3:1 mixture of concentrated  $\text{H}_2\text{SO}_4$  (98%) and  $\text{HNO}_3$  (69%) at 70°C for 4 h (18–20) and filtered through a 10- $\mu$ m pore size PTFE filter paper.  
Or

Pristine MWCNTs were refluxed in 4 M  $\text{HNO}_3$  for 24 h and filtered through a 10- $\mu\text{m}$  pore size PTFE filter paper.

2. After filtration, the refluxed MWCNTs were exposed to 1 M HCl and sonicated for about 30 min.
3. The carboxylated MWCNTs were filtered, and washed with deionized water and dried in air.

### **3.2. Amidation**

1. MWCNT-COOH and mouse monoclonal IgG was mixed in a tube at the ratio 1:10.
2. A mixture solution of 0.40 M 1-ethyl-3-(3-dimethyl-amino-propyl) carbodiimide (EDC) and 0.10 M *N*-hydroxy succinimide (NHS) was added to initiate cross-linking reactions between carboxyl groups on MWCNTs and amine groups in IgG.
3. The reaction tubes were rotated at room temperature for 1 h.
4. After centrifugation and decanting supernate, mouse IgG functionalized MWCNTs were re-suspended in PBS buffer.

### **3.3. TEM Characterization**

1. 5  $\mu\text{L}$  of dilute aqueous sample was spotted onto a grid and left for 90 s.
2. Lightly touch one edge of the grid with filter paper to wipe off moisture.
3. Grids were then allowed to air dry prior to analysis.
4. TEM: Observe the samples on grids in electron microscopy with an accelerating voltage of 120 kV. Figure 1 shows the results obtained.

### **3.4. XPS Measurements (See Notes 3 and 4)**

1. Parameter setting:
  - (a) Pressure ranges are as follows:  $2 \times 10^{-6}$  mbar (fast entry chamber),  $4 \times 10^{-8}$  mbar (preparation chamber), and  $4 \times 10^{-9}$  mbar (sample analysis chamber).
  - (b) High transmission FAT mode, 14.12 keV, 25 mA, Al  $K\alpha$  (1,486.7 eV), was used for the analysis at 90° electron take off angle for normal non-charging samples (45° for the charging samples).
  - (c) The analyzer slit width was set for 0.8 mm, and the resulting overall energy resolution was 0.35 eV.
2. The SCIENTA software was used for data acquisition and data analysis.
3. The binding energy of the C1s of graphite, 284.5 eV ( $\pm 0.35$  eV energy resolution of the spectrometer at the settings employed) was taken as the reference.
4. Prior to individual elemental scans, a survey scan was taken for all the samples in order to detect the elements present.

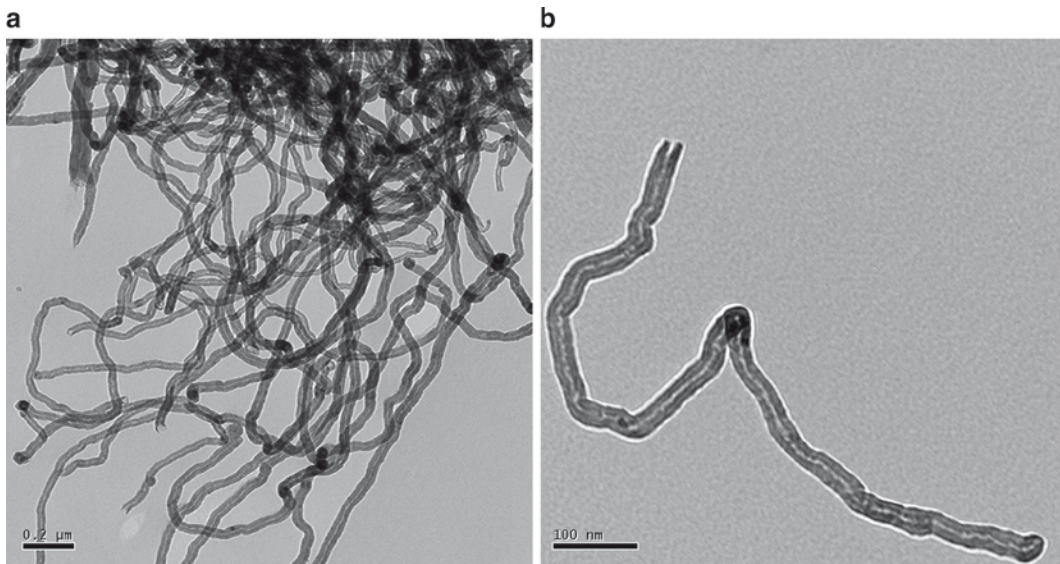


Fig. 1. (a) and (b) TEM images of the carboxylated MWCNTs

5. The obtained XPS spectra of CNT-protein adduct are listed in Fig. 2. The C1s XPS of the oxidized nanotubes in Fig. 2a shows a large peak at 284.4 eV from the nanotubes, a smaller peak at 286.4 eV, and a well-separated peak at 288.8 eV. The peak at 288.8 eV is attributed to the carbonyl group in the carboxylic acid group. The peak at 286.4, 2 eV higher than the main peak, is attributed to C atoms in ether-like linkages. The corresponding N(1s) spectrum shows no signal above the detection limit of the instrument, even with extensive signal averaging. After conjugation with proteins, the modified tubes were characterized by XPS after briefly warming to 75°C in an ultrahigh vacuum to remove any residual physically adsorbed proteins. Compared to the main bulk C1s at 284.4 eV, the resulting C1s photoelectron spectrum shows some narrowing of the bulk peak (Fig. 2b). We notice that there is no significant intensity near 288.8 eV. The absence of intensity at 288.8 eV is important because the C1s binding energy of carboxylic groups is expected to decrease significantly when a carboxylic acid group is converted to a carbonyl amide, which is at 288.45 eV. Carbon atoms in carboxylic acid groups and in carbonyl amide groups typically have C1s binding energies ~4.0 eV and ~3.0 eV higher, respectively, than C atoms in alkanes (21). Thus, the changes we observe in the C1s spectrum support the formation of a carbonyl amide linkage to the nanotubes. The N1s spectrum shows a peak

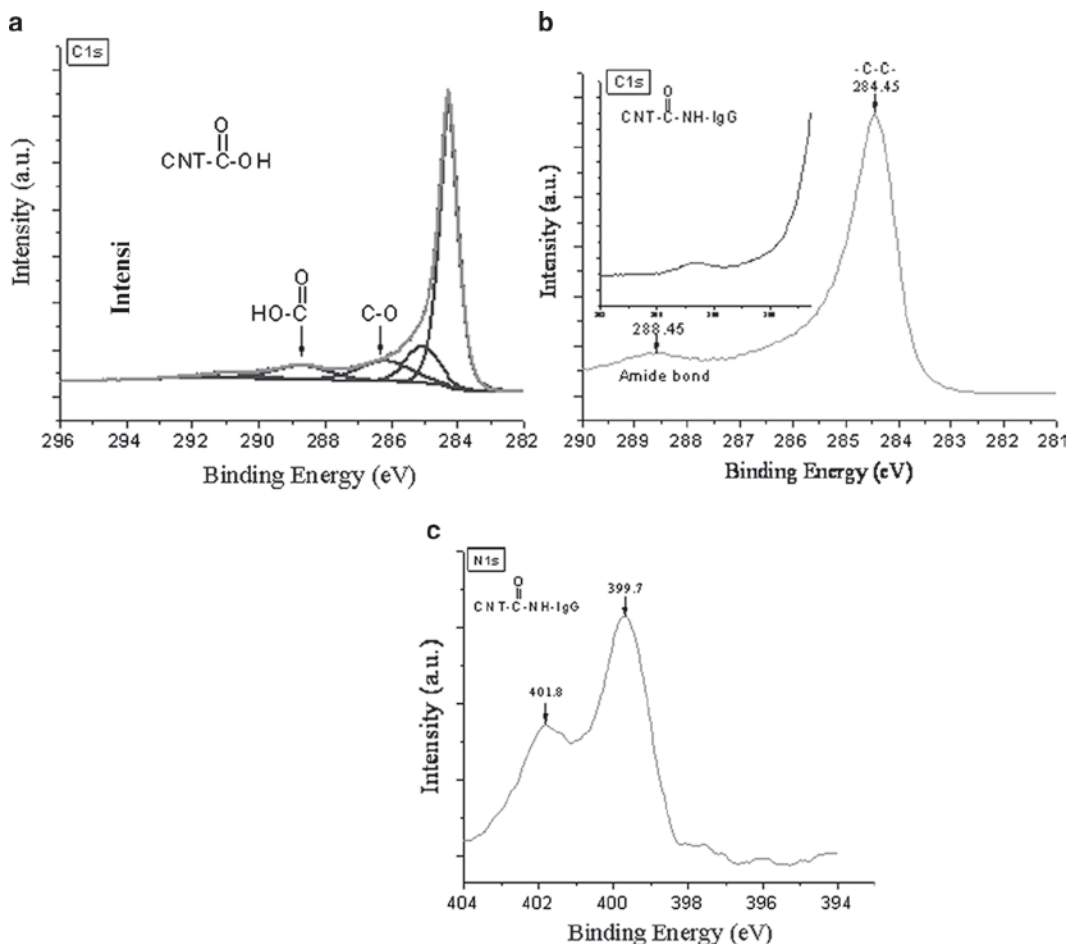


Fig. 2. XPS of chemically modified CNTs. C1s spectrum of CNT-COOH (a); C1s spectrum of protein functionalized CNTs (b), showing elimination of the carboxylic peak and increased peak from the amide group. N1s spectrum of protein functionalized MWCNTs (c)

with a binding energy of 399.7 eV (Fig. 2c). Previous studies have shown that amides have binding energies in the range of ~399.5–400.2 eV (21). Therefore, the peak energies are consistent with the formation of the amide bonds.

### 3.5. ATR-FTIR Measurements (See Notes 5 and 6)

1. Sample preparation: MWCNT-protein adducts were grinded to a fine powder.
2. Sample loading: The ZnSe through top-plate of the horizontal ATR was covered by a fine layer of the grinded sample, avoiding air bubble formation on the crystal surface.
3. Parameters setting: A detector gain of 1 and a speed of the moving mirror of 0.6  $\text{cm}^{-1}$  were employed.

4. Spectra measurements: The spectra were obtained in the absorbance mode from 4,000 to 700  $\text{cm}^{-1}$  by accumulating 100 scans, working with a spectral resolution of 2  $\text{cm}^{-1}$ .
5. Control: Absorbance spectra were corrected versus a spectrum of distilled water, obtained in the same instrumental conditions.
6. Figure 2.3 shows the typical ATR-FTIR spectra of MWCNT-COOH before and after functionalization by IgG. The absorption peak at 1,569  $\text{cm}^{-1}$  indicates the presence of amide bond which comes from the covalent linkage between CNTs and IgG through the functional groups.

### 3.6. AFM Measurements

1. MWCNT-protein adducts suspension: Suspend MWCNT-protein adducts in PBS to a concentration of 1 mg/mL. This concentration provides convenient coverage for AFM imaging and may be used for a variety of similar size samples.
2. Prepare mica: Cleave a fresh mica surface by first pressing some adhesive tape against the top mica surface, then peeling off the tape. Glue mica to a small puck (e.g., using epoxy).
3. Deposit sample solution on mica: Deposit 50  $\mu\text{L}$  of protein solution on the freshly cleaved mica.
4. Sample to bind to substrates: Allow 20–30 min for the sample to bind to the mica substrate. Binding time may vary with different samples (it can be up to 24 h).
5. Rinse unbound sample: Rinse the sample with a large quantity of buffer to remove unbound protein.
6. AFM measurements: AFM measurements were performed under ambient conditions using a NanoScope V Controller

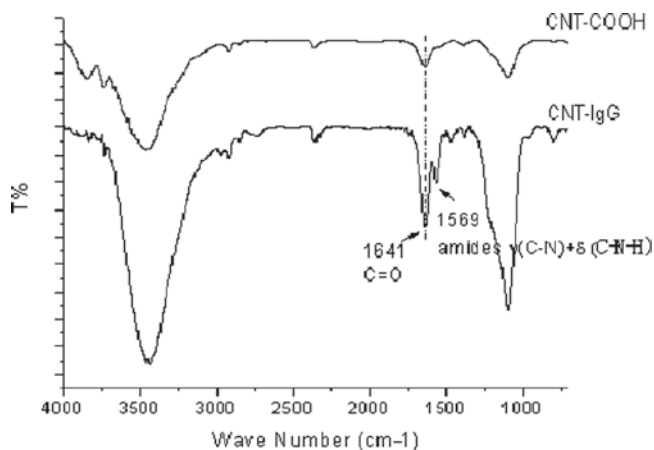


Fig. 3. ATR-FTIR spectra of CNTs. The absorption peak at 1,569  $\text{cm}^{-1}$  indicates the presence of amide linkage between MWCNTs and IgG

with a multimode atomic force microscope in tapping mode with standard 125 mm single-crystal silicon cantilevers.

7. Figure 4 shows the herein obtained AFM images: MWCNTs appear as bright lines in the image and the circle particles represent bound proteins. Proteins are connected to the side-wall of nanotubes, indicating that oxidation took place in the defect sites of sidewalls. From the observations of several samples, we conclude that protein attachment mainly occurred at nanotube sidewalls, because chemical functionalization occurred primarily at the sidewalls. This AFM image is similar to that of cytochrome *c*-functionalized purified SWCNTs which was taken by Davis and co-workers (14).

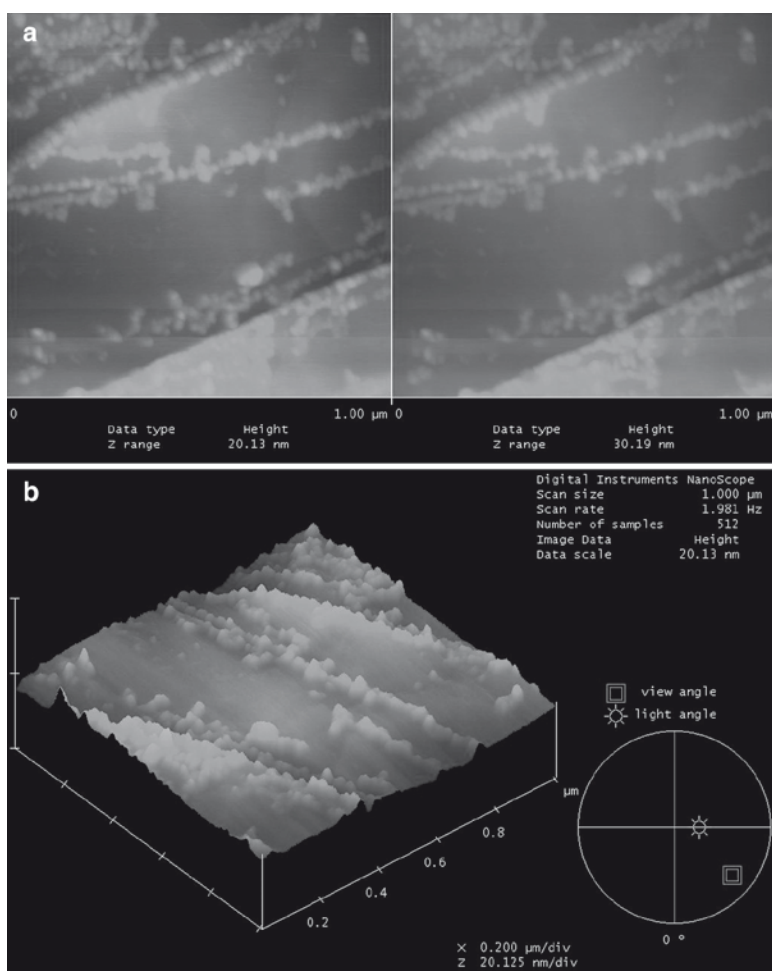


Fig. 4. (a) and (b) AFM (tapping mode) images of protein-MWCNT adducts. MWCNTs appear as *bright lines* and the *circle particles* represent bound proteins



---

## 4 Notes

1. Unless stated otherwise, water used in this protocol was Milli-Q deionized water.
2. Unless stated otherwise, the CNT suspensions should be prepared in D.I water and followed by ultrasonication for 30 min.
3. Use only polyethylene gloves. Other gloves may contain silicones that can contaminate the surface.
4. Make sure everything, used to handle or store your samples, is clean (tweezers, etc.). It is recommended to have a dedicated set of clean tools for handling your samples. In particular, take care to avoid grease, oils, and silicone contaminants around your tools and work area. A general cleaning protocol that often works is to clean the utensils that will handle samples with the following solvents (in this order): Hexanes, Methylene chloride, Methanol, and Acetone.
5. The sample must be in direct contact with the ATR crystal, because the evanescent wave or bubble only extends beyond the crystal 0.5–5  $\mu\text{m}$ .
6. The refractive index of the crystal must be significantly greater than that of the sample or else internal reflectance will not occur – the light will be transmitted rather than internally reflected in the crystal.

---

## Acknowledgments

The financial support of Key Laboratory Funding Scheme of Shenzhen Municipal Government, BTC operation fund (CityU project No. 9683001) and City University of Hong Kong (Project No. 7002100) are gratefully acknowledged.

## References

1. Loo C, Hirsch L, Lee MH, Chang E, West J, Halas N, Drezek R (2005) Gold nanoshell bioconjugates for molecular imaging in living cells. *Opt Lett* 30:1012–1014
2. Medintz IL, Uyeda HT, Goldman ER, Mattoussi H (2005) Quantum dot bioconjugates for imaging, labelling and sensing. *Nat Mater* 4:435–446
3. Lewis JD, Destito G, Zijlstra A, Gonzalez MJ, Quigley JP, Manchester M, Stuhlmann H (2006) Viral nanoparticles as tools for intravital vascular imaging. *Nat Med* 12:354–360
4. Loo C, Lowery A, Halas N, West J, Drezek R (2005) Immunotargeted nanoshells for integrated cancer imaging and therapy. *Nano Lett* 5:709–711



5. Kam NWS, O'Connell M, Wisdom JA, Dai HJ (2005) Carbon nanotubes as multifunctional biological transporters and near-infrared agents for selective cancer cell destruction. *Proc Natl Acad Sci USA* 102:11600–11605
6. Pantarotto D, Briand JP, Prato M, Bianco A (2004) Translocation of bioactive peptides across cell membranes by carbon nanotubes. *Chem Commun* 16–17
7. Kam NWS, Jessop TC, Wender PA, Dai HJ (2004) Nanotube molecular transporters: internalization of carbon nanotube-protein conjugates into mammalian cells. *J Am Chem Soc* 126:6850–6851
8. Connolly S, Fitzmaurice D (1999) Programmed assembly of gold nanocrystals in aqueous solution. *Adv Mater* 11:1202–1205
9. Caswell KK, Wilson JN, Bunz UHF, Murphy CJ (2003) Preferential end-to-end assembly of gold nanorods by biotin-streptavidin connectors. *J Am Chem Soc* 125:13914–13915
10. Lee JA, Govorov AO, Dulka J, Kotov NA (2004) Bioconjugates of CdTe nanowires and Au nanoparticles: Plasmon-exciton interactions, luminescence enhancement, and collective effects. *Nano Lett* 4:2323–2330
11. Lee J, Govorov AO, Kotov NA (2005) Bioconjugated superstructures of CdTe nanowires and nanoparticles: multistep cascade Forster resonance energy transfer and energy channeling. *Nano Lett* 5:2063–2069
12. Wang S, Mamedova N, Kotov NA, Chen W, Studer J (2002) Antigen/antibody immunocomplex from CdTe nanoparticle bioconjugates. *Nano Lett* 2:817–822
13. Srivastava S, Verma A, Frankamp BL, Rotello VM (2005) Controlled assembly of protein-nanoparticle composites through protein surface recognition. *Adv Mater* 17:617–621
14. Azamian BR, Davis JJ, Coleman KS, Bagshaw CB, Green MLH (2002) Bioelectrochemical single-walled carbon nanotubes. *J Am Chem Soc* 124:12664–12665
15. Shim M, Kan NWS, Chen RJ, Dai HJ (2002) Functionalization of carbon nanotubes for biocompatibility and biomolecular recognition. *Nano Lett* 2:285–288
16. Chen WW, Tzang CH, Tang JX, Yang MS, Lee ST (2005) Covalently linked deoxyribonucleic acid with multiwall carbon nanotubes: synthesis and characterization. *Appl Phys Lett* 86:103114
17. Sarah EB, Cai W, Lasseeter TL, Weidkamp KP, Hamers RJ (2002) Covalently bonded adducts of deoxyribonucleic acid (DNA) oligonucleotides with single-wall carbon nanotubes: synthesis and hybridization. *Nano Lett* 2:1413–1417
18. Yi CQ, Fong CC, Zhang Q, Lee ST, Yang MS (2008) The structure and function of ribonuclease A upon interacting with carbon nanotubes. *Nanotechnology* 19:095102
19. Yi CQ, Fong CC, Chen WW, Qi SJ, Tzang CH, Lee ST, Yang MS (2007) Interactions between carbon nanotubes and DNA polymerase and restriction endonucleases. *Nano technology* 18:025102
20. Zhang DW, Yi CQ, Zhang JC, Chen Y, Yao XS, Yang MS (2007) Effects of carbon nanotubes on the proliferation and differentiation of primary osteoblasts. *Nanotechnology* 18:475102
21. Moulder JF, Stickley WF, Sobol PE, Bomben KD (1992) Handbook of X-ray photoelectron spectroscopy. Perkin-Elmer, Eden Prairie, MN

Carbon Nanotubes

Methods and Protocols

Balasubramanian, K.; Burghard, M. (Eds.)

2010, XI, 254 p., Hardcover

ISBN: 978-1-60761-577-4

A product of Humana Press